

Passenger Car Active Braking System: Model and experimental validation (Part I)

Original

Passenger Car Active Braking System: Model and experimental validation (Part I) / Tota, Antonio; Galvagno, Enrico; Velardocchia, Mauro; Vigliani, Alessandro. - In: PROCEEDINGS OF THE INSTITUTION OF MECHANICAL ENGINEERS. PART C, JOURNAL OF MECHANICAL ENGINEERING SCIENCE. - ISSN 0954-4062. - STAMPA. - 232:4(2018), pp. 585-594. [10.1177/0954406216686388]

Availability:

This version is available at: 11583/2674329 since: 2018-05-21T12:40:58Z

Publisher:

LONDON:SAGE PUBLICATIONS LTD

Published

DOI:10.1177/0954406216686388

Terms of use:

This article is made available under terms and conditions as specified in the corresponding bibliographic description in the repository

Publisher copyright

(Article begins on next page)

Passenger Car Active Braking System: model and experimental validation (Part I)

Antonio Tota, Enrico Galvagno, Mauro Velardocchia, and Alessandro Vigliani

antonio.tota@polito.it, enrico.galgagno@polito.it, mauro.velardocchia@polito.it, alessandro.vigliani@polito.it

Abstract

The paper proposes a method to characterize the dynamic behavior of a normal production hydraulic brake system through experiments on a hardware-in-the-loop (HIL) test bench for both modeling (Part I) and control (Part II) tasks.

The activity is relative to analyze, model and control ABS/ESC digital valves, aiming at obtaining reference tracking and disturbance-rejection performance similar to that achievable when using pressure proportional valves.

The first part of this two-part study is focused on the development of a mathematical model which emulates the pressure dynamics inside brake caliper when inlet valve, outlet valve and motor-pump are controlled by a digital or PWM signal. The model takes into account some inherent non-linearities of these systems, e.g. the variation of fluid bulk modulus with pressure while inlet and outlet valves together with the relay box are modeled as second order systems with variable gains.

The HIL test rig is used for both parameters identification and model validation, which will be used for control strategy development presented in the second part of this research activity.

Index Terms

ABS test bench, brake hydraulic systems, dynamic system modeling, valve dynamics.

I. INTRODUCTION

Anti-lock brake systems (ABS) have been used all over the years to ensure vehicle safety and grant directional control. The fundamental task is to prevent wheel from locking thus exploiting the maximum available adhesion coefficient by keeping the slip ratio within an appropriate range [1], [2].

Different control techniques aiming at regulating wheels slip [3], [4], [5], [6] can be found in the literature and most of them are designed and tuned on mathematical or numerical models of the hydraulic braking system more or less able to describe its behavior. In [7] a nonlinear model based on physical laws of braking system is built receiving as input the brake pedal force and generating as output the wheel braking torque in order to design PWM and switching controls to be compared with a normal production ABS ECU by using a HIL test bench. The model takes into account some simplifications i.e. considering the TMC as a hydraulic cylinder with a single mass, and it is not experimentally validated in open loop. A bond graph method for modeling the components of a commercial brake system is evaluated in [8]. Ozdalyan and Blundell [9] present the application of ADAMS to model and simulate the performance of an anti-lock braking system in order to investigate the interaction between the tyre and the ABS system. Important factors influencing the hysteresis pressure losses in a hydraulic brake system

are analyzed in [10] while a methodology for estimating the flow coefficient as a function of the Reynolds number is presented in [11] by exploiting a parametric CFD simulations of the flow rate in hydraulic valve systems. A first order model with the same time constants for increase and decrease mode is presented in [12]. The values of these parameters are unknown and no justifications are reported to consider them constant. The paper presented by Moaveni in [13] identifies single-input (pressure of master cylinder) single-output (brake calipers pressure) linear minimum-order models for the hydraulic unit in the increase and decrease mode by employing the experimental data of a test automobile and using least-square method and prediction error method. Raza et al. [14] experimentally validated a dynamic model by testing a laboratory set up also used for identifying a first-order non-linear model. They used the brake pedal force as input of the model and the master cylinder pressure line as the output variable. A non-linear model of a PWM-driven pneumatic fast switching valve is presented in [15] where unknown parameters are identified by using direct search optimization; model validation is carried out by comparing model results with experimental test.

The present work aims at developing a non-linear model for simulating and estimating the braking system dynamics by introducing an identification methodology from experimental measurements. This methodology and the non-linear model can be applied for different braking systems. The model is experimentally validated and is able to receive as input a PWM voltage signal which is commonly used as a control output of the strategies available in the literature. The non-linear model presented in the paper is not intended to be used for control design tasks but for system dynamic description and analysis; in part II of this research, a linearized version of this non-linear model is derived in order to design a proper closed loop controller.

Model inputs are the TMC rod position and the command for each inlet/outlet valve together with the activation of Motor-Pump while output variables are TMC and brake calipers pressures. A procedure for a practical parameters identification in order to adapt the same model to different brake systems is also presented. The model takes into consideration the non-linearities that can influence the dynamics of relevant variables like pressures and flow rates. Inlet and outlet valve are modeled as second order transfer functions, whose static gain depends on the Duty Cycle of input voltage signal. A Braking HIL Test Rig, similar to the one presented in [16], is built for control and validation tasks. The correlation between the valves effective flow area and the Duty Cycle of PWM signal at constant frequency applied to inlet/outlet electrovalves is experimentally evaluated and will be further investigated in the second part of this research based on the development of a continuous braking control strategy.

The paper is divided into six sections including the introduction: Braking HIL test rig, used for model identification and validation, is described in section II; Section III is related to the description of the mathematical model used to simulate the dynamic behavior of oil pressure inside a normal production braking unit; Section IV presents the method used for identifying all model parameters and section V shows experimental validation of non-linear model. Finally some conclusions are reported in section VI.

II. BRAKING HIL TEST RIG

The HIL test rig shown in Fig. 1 includes a hydraulic braking system composed of a tandem master cylinder (TMC), a customized ABS/ESC hydraulic unit and four brake calipers located on non-rotating disks. A hydraulic power unit using a

double effect cylinder with flow proportional valve emulates the brake pedal action. The ECU of ABS/ESC system is customized to get a direct command to the motor-pump and to each single valve by means of digital control signals.

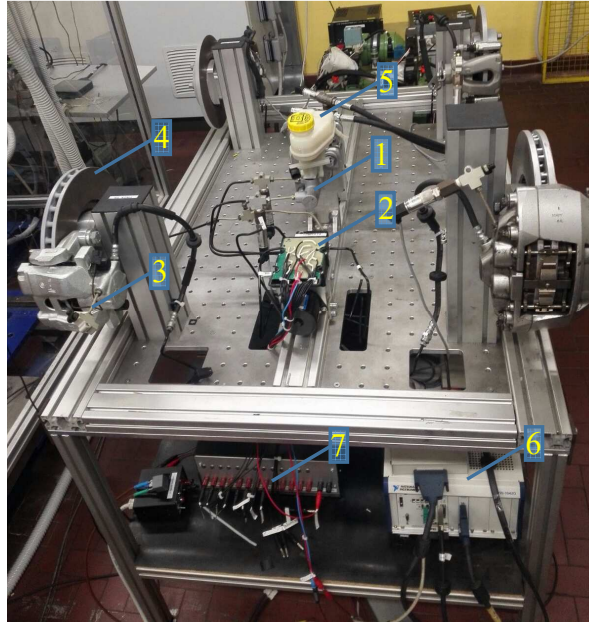


Fig. 1. HIL Test Rig 1-TMC 2-customized ESC 3-Brake caliper 4-Brake disk 5-oil tank 6-Data Acquisition System 7-Relay Box

Valves and motor-pump solenoids are powered by a 12 V DC line through solid state relays, one for each of the twelve valves and one for the motor-pump. Relays control signals can be equal to 5 V (relay 'On') or 0 V (relay 'Off') according to TTL logic levels.

The bench is equipped with a set of sensors necessary for monitoring and control:

- 8 pressure sensors: one for each brake caliper (4), one for each TMC chamber (2) and one for each brake pedal cylinder chamber (2)
- 1 potentiometer for double-effect hydraulic cylinder rod position.

A model of the hydraulic system was developed in Matlab[®]/Simulink[®] while a real time system manages the data acquisition process and the deployment of the system model together with its control logic. In particular, experiments are handled by using:

- NI Labview[®] Real-Time for data acquisition and system identification processes
- NI Veristand[®] NI for control and hardware-in-the-loop tasks

The real time system enables to send control signals to each valve and motor-pump by using a digital board together with the relays-box.

In this configuration, a model of the system based on experimental data has been realized in order to evaluate its accuracy with respect to the real system and/or to design suitable control logic.

III. MATHEMATICAL MODEL

The simplified scheme of hydraulic circuit composed by the TMC, inlet and outlet valves and front/rear brake calipers is represented in Fig. 2. The hydraulic connections between the two TMC chambers with the four calipers is typical of a 'X' scheme, where the first chamber delivers oil to Front Left (FL) and Rear Right (RR) calipers meanwhile the second chamber delivers oil to Front Right (FR) and Rear Left (RL) calipers. Since the paper is concentrated on the pressure dynamics inside one brake caliper (i.e. RR brake caliper), the FR-RL hydraulic behavior is represented by an equivalent hydraulic circuit.

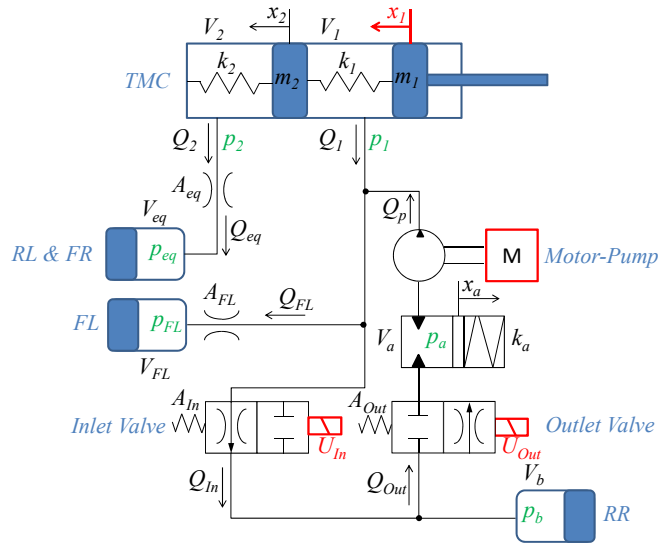


Fig. 2. Representation of ABS/ESC hydraulic circuit with input (red) and output (green)

The TMC axial dynamics can be described as a 2 d.o.f (displacements x_1 and x_2) system but since x_1 represents an input, a unique equation is sufficient to describe the motion of the system:

$$m_2\ddot{x}_2 + F_{f2}\text{sgn}\dot{x}_2 - b_1(\dot{x}_1 - \dot{x}_2) + b_2\dot{x}_2 - k_1(x_1 - x_2) + k_2x_2 = (p_1 - p_2)S \quad (1)$$

where k_i is the stiffness of the i_{th} spring, m_i the mass of i_{th} element, b_i the oil viscous damping coefficient of the i_{th} chamber, F_{f2} the Coulomb friction coefficient, S the hydraulic cylinder surface and p_i the pressure inside the i_{th} chamber of TMC.

The spring hydraulic accumulator is modeled as a 1 d.o.f (piston displacement x_a) dynamic system:

$$m_a\ddot{x}_a + b_a\dot{x}_a + F_{fa}\text{sign}\dot{x}_a + k_ax_a = p_aS_a \quad (2)$$

where $k_a, m_a, b_a, F_{fa}, S_a$ and p_a are respectively the stiffness, mass, viscous damping coefficient, Coulomb friction coefficient, cylinder surface and oil pressure in the spring accumulator.

The two ports of the TMC and each valve orifice can be considered as hydraulic resistances, so flow rates Q can be calculated respectively as :

$$\left\{ \begin{array}{lcl} Q_{In} & = & c_{q,In} A_{In} \sqrt{\frac{2|p_1 - p_b|}{\rho}} \operatorname{sgn}(p_1 - p_b) \\ Q_{Out} & = & c_{q,Out} A_{Out} \sqrt{\frac{2|p_b - p_a|}{\rho}} \operatorname{sgn}(p_b - p_a) \\ Q_{FL} & = & c_{q,FL} A_{FL} \sqrt{\frac{2|p_1 - p_{FL}|}{\rho}} \operatorname{sgn}(p_1 - p_{FL}) \\ Q_{eq} = Q_2 & = & c_{q,eq} A_{eq} \sqrt{\frac{2|p_2 - p_{eq}|}{\rho}} \operatorname{sgn}(p_2 - p_{eq}) \\ Q_1 & = & Q_{In} + Q_{FL} - Q_p \end{array} \right. \quad (3)$$

where Q_i is the flow rate through the i_{th} element and A_i the flow area of the i_{th} component (see Fig. 2). The flow coefficient $c_{q,i}$ depends on the pressure drop Δp across the hydraulic resistance [17]:

$$c_{q,i} = c_{q,max} \tanh\left(2 \frac{\lambda}{\lambda_{cr}}\right) \quad (4)$$

$$\lambda = \frac{h_d}{\nu} \sqrt{\frac{2|\Delta p|}{\rho}} \quad (5)$$

where h_d is the hydraulic diameter, ν the kinematic viscosity, ρ the oil density, $c_{q,max}$ the maximum value of the flow coefficient at which it asymptotically approaches for $\lambda \gg \lambda_{cr}$; λ_{cr} is the critical flow number at which transition from laminar to turbulent flows occurs.

The 2 TMC chambers are modeled as variable volume hydraulic capacities, while brake calipers as fixed volume capacities by means of the following equation:

$$\frac{dp_i}{dt} = \frac{\beta_i}{V_i} (\pm Q_i - \dot{V}_i) \quad (6)$$

where $i = 1, 2, FL, eq$ and flow rate is positive when it flows inside the volume V_i . β is the bulk modulus of hydraulic fluid and it is considered a function of pressure p_i :

$$\beta_i = \beta_n \frac{1 + \alpha \left(\frac{p_{atm}}{p_{atm} + p_i}\right)^{1/n}}{1 + \alpha \frac{(p_{atm})^{1/n}}{n(p_{atm} + p_i)^{\frac{n+1}{n}}} \beta_n} \quad (7)$$

where α is the relative gas content at atmospheric pressure p_{atm} , β_n is the pure liquid bulk modulus and n is the gas-specific heat ratio.

Similarly, the dynamics of brake caliper pressure p_b and spring accumulator pressure p_a are respectively evaluated by :

$$\frac{dp_b}{dt} = \frac{\beta_b}{V_b} (Q_{In} - Q_{Out} - \dot{V}_b) \quad (8)$$

$$\frac{dp_a}{dt} = \frac{\beta_a}{V_a} (Q_{Out} - Q_p - \dot{V}_a) \quad (9)$$

The TMC chambers may change their volumes due to the displacements of the two pistons:

$$V_2 = V_{20} - Sx_2 \quad (10)$$

$$V_1 = V_{10} + S(x_2 - x_1) \quad (11)$$

with V_{10} and V_{20} respectively the initial value of the first and second chamber of the TMC when no forces are applied.

The variation of volumes V_{FL}, V_{eq} and V_b , are neglected, i.e.: $\dot{V}_{FL} \approx 0, \dot{V}_{eq} \approx 0, \dot{V}_b \approx 0$ (fixed volume hydraulic chambers).

Volumes V_{eq} , V_{FL} and flow areas A_{eq} , A_{FL} are related to V_b and A_{In} by the following equations:

$$\begin{cases} V_{FL} &= q_{FL} V_b \\ V_{eq} &= V_{FL} + V_b \\ A_{FL} &= A_{In} \\ A_{eq} &= 2A_{In} \end{cases} \quad (12)$$

where coefficient q_{FL} represents the proportional relation between front hydraulic cylinders volume and rear one.

The flow rate generated by the pump Q_p is influenced by the spring accumulator pressure p_a since when the intake pressure is too low the motor-pump is unable to deliver any flow rate:

$$Q_p = Q_{ss} [1 - e^{-3p_a/p_{th}}] \quad (13)$$

where Q_{ss} is the steady-state value of flow rate delivered by motor-pump and p_{th} represents the pressure threshold at which the flow rate drops to zero.

Finally, inlet and outlet valves dynamics are modeled with a cascade series of time delays and a second-order transfer functions with non constant static gain which is a function of PWM DC of input signal:

$$\frac{A_i(s)}{U(s)} = \frac{G_s}{\frac{s^2}{\sigma_n^2} + \frac{2\zeta s}{\sigma_n} + 1} \quad (14)$$

where s is the Laplace variable, A_i the effective inlet/outlet flow area, U is the input solenoids valve (Voltage), G_s is the static gain, σ_n is the system natural frequency and ζ is its damping ratio.

The model inputs for the model are the position of TMC rod x_1 (which represents the brake pedal position in a common passenger car) together with the command signal for inlet, outlet valves and motor-pump while the outputs are the pressures of each brake calipers, the pressures of the two TMC chambers and x_2 .

IV. MODEL PARAMETERS IDENTIFICATION

All the parameters introduced by equations 1-14 and reported in table I have been either measured, extracted from technical specifications or experimentally estimated.

Masses m_2 , m_a spring stiffness k_2, k_a and cylinder surfaces S, S_a have been measured from the technical drawings. Oil density ρ and kinematic viscosity ν have been derived from DOT 4 brake fluid properties; The parameters characterizing the oil flow through an orifice like maximum flow coefficient $c_{q,max}$, and critical flow number λ_{cr} are reported in table I. These coefficients are supposed constant and not subjected to parameter identification.

The Bulk modulus variations are modeled with the non-linear relation described by Eq. 7 [18]. β_n and α are identified in order to describe the non-linear dependence by oil pressure of bulk modulus which heavily influences pressure dynamics: in

Fig. 3 the effect of a step change of the inlet control signal, from fully closed to fully open, considering a null initial brake pressure is shown. In the meanwhile TMC rods moves from the initial position to a final steady state position. Different values of β_n and α are tested in simulation in order to find optimal values to match the experimental trend (reported in table I). All experimental pressure trends measured by sensors have been filtered with a digital zero-phase filter characterized by a cut-off frequency of 50 Hz in order to better highlight the comparison with simulation results where high frequency contents are not modeled.

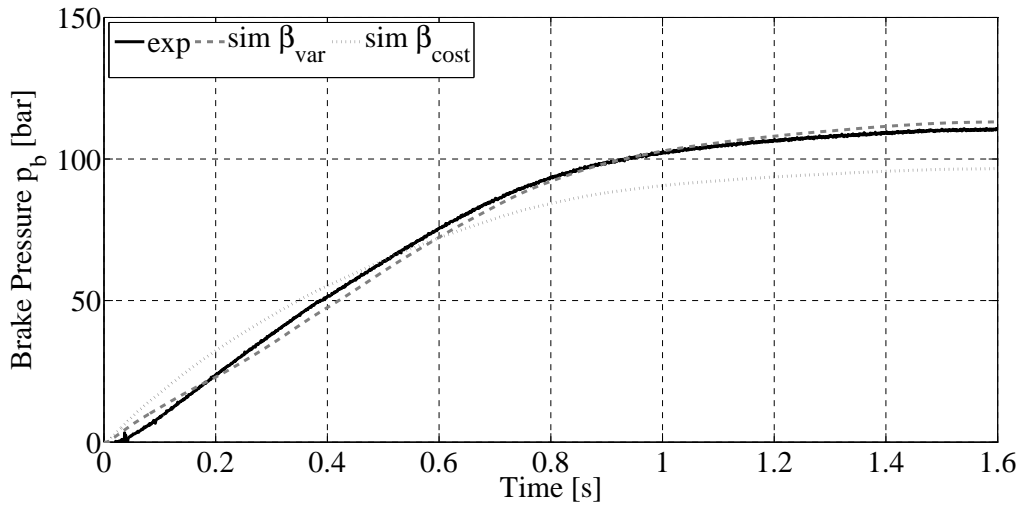


Fig. 3. Influence of Bulk modulus on brake pressure trend: experimental (solid black line) vs simulation with constant β (dotted gray line) and with non-linear β (dashed gray line)

Eq. 6 states that pressure derivative depends on volume V_i , and on total flow rate Q_i entering or exiting the volume V_i . Effective values of valves flow area A_i and chambers volume V_{i0} , V_i together with unknown damping coefficients b_2, b_a and friction forces F_{f2}, F_{fa} have been experimentally identified through the following tests: the starting steady-state condition is when the TMC rod is pushed until TMC pressures p_1, p_2 reach a desired initial values (i.e. 130 bar) with inlet valves completely open and outlet valves completely closed (which represents their normal configuration). From this initial condition, the RR inlet valve is closed and the RR outlet valve is opened together with the activation of the motor-pump, thus emptying the RR brake caliper (falling phase). Once all pressures have stabilized, the outlet valve is closed with the motor-pump switched off and the inlet valve is opened, thus filling the RR brake caliper (raising phase).

The 'raising phase' is used to identified volumes V_b, V_{FL}, V_{eq} of each brake caliper, initial TMC volumes V_{01}, V_{02} and flow areas A_{In}, A_{FL}, A_{eq} . By a curve-fitting procedure between the time history of simulated pressures p_1, p_2, p_{eq}, p_{FL} and p_b and their experimental values, it has been possible to identify the parameters $V_b, q_{FL}, A_{In}, V_{01}$ and V_{02} . Fig. 4 shows the comparison between experimental data and simulation results considering the best combination of unknown parameters. Volumes V_b and V_{0i} influence the steady-state values at which all pressures tend after an initial transient phase which is mainly characterized by A_{In} .

Effective values of unknown damping coefficient b_2 and friction force F_{f2} cannot be easily identified from experimental data since position x_2 is not measured. Reasonable values are chosen for simulations and a post-processing analysis of their influence

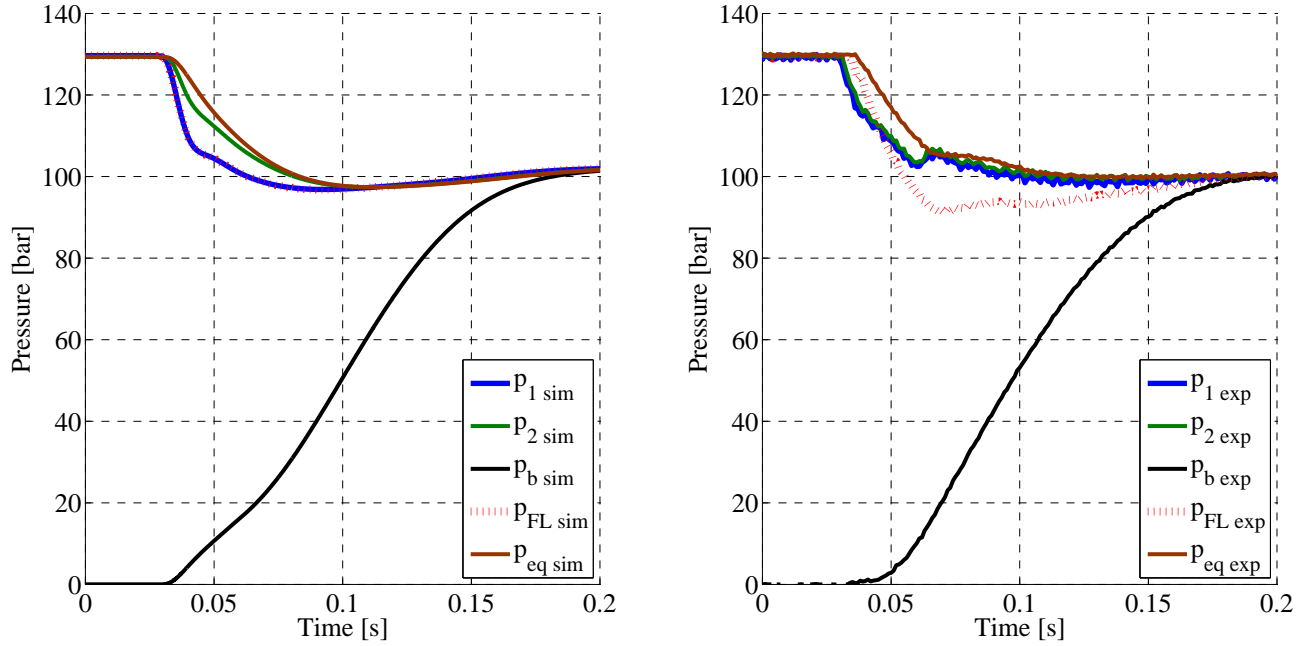


Fig. 4. 'Raising phase': 1= 1° chamber TMC, 2= 2° chamber TMC, b= Rear Right caliper, FL= Front Left caliper, eq= equivalent Front Right+Rear Left caliper, exp=experimental, sim= simulation

on pressure dynamics is reported in Fig. 5 where it is possible to understand how b_2 influences the transient behavior while F_{f2} affects the steady-state value of TMC and brake pressures. More specifically, an increase of b_2 causes a larger transient pressure difference between the two TMC chambers and a slower response of inlet valve without affecting steady-state behavior. An increase of F_{f2} provokes a steady-state pressure difference between the two TMC chambers without modifying considerably the valve transient phase.

The 'falling phase' is used to identify remaining parameters characterizing the pressure dynamics inside the discharge hydraulic branch composed by the outlet valve, the spring accumulator and the motor-pump. Q_{ss} , p_{th} and A_{Out} have been identified through a curve fitting procedure between experimental and simulated pressures as shown in Fig. 6:

Q_{ss} is strictly related to the TMC pressure gradients while the flow area A_{Out} influences both brake and accumulator pressure gradients. After 0.3 seconds, the flow rate delivered by the motor-pump decrease from Q_{ss} to 0 because accumulator pressure is too low: it is important to underline the effect of one way valve inside the discharge branch which prevents oil to flow-back to the brake caliper.

Inlet and outlet valves can be controlled by applying a digital ON/OFF voltage command to their solenoids through the relay box. An overall analysis about valves dynamical behavior has been carried out by applying a PWM signal to their solenoids in order to identify transient and steady state characteristics.

Fig. 7 refers to the non-linear behavior of inlet valve when a PWM voltage command with frequency of 900 Hz and different Duty Cycle (DC) is applied to its solenoid.

It is possible to observe a clear dependence of the pressure gradient on the Duty Cycle. This behavior represents the transformation from the PWM digital command to the effective flow area A_i through the relay box and electro-valves. This

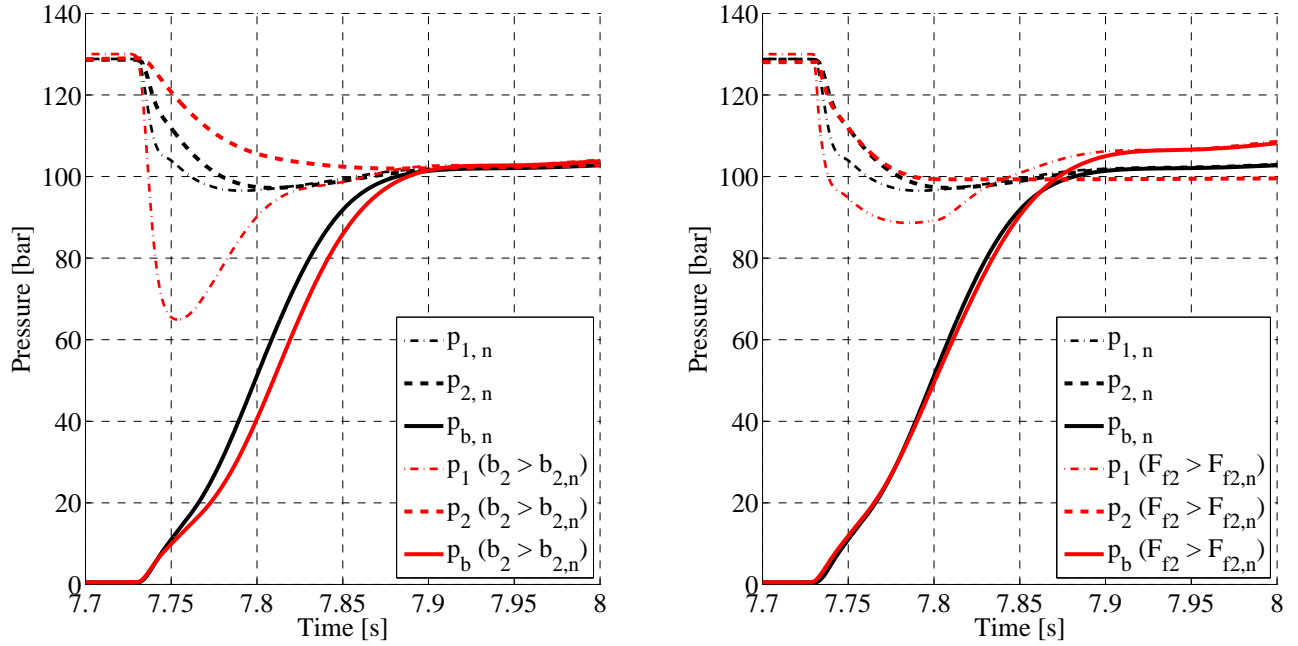


Fig. 5. Sensitivity analysis on b_2 and F_{f2} : 1= 1st TMC chamber, 2= 2nd TMC chamber, b= Rear Right caliper, n = nominal condition

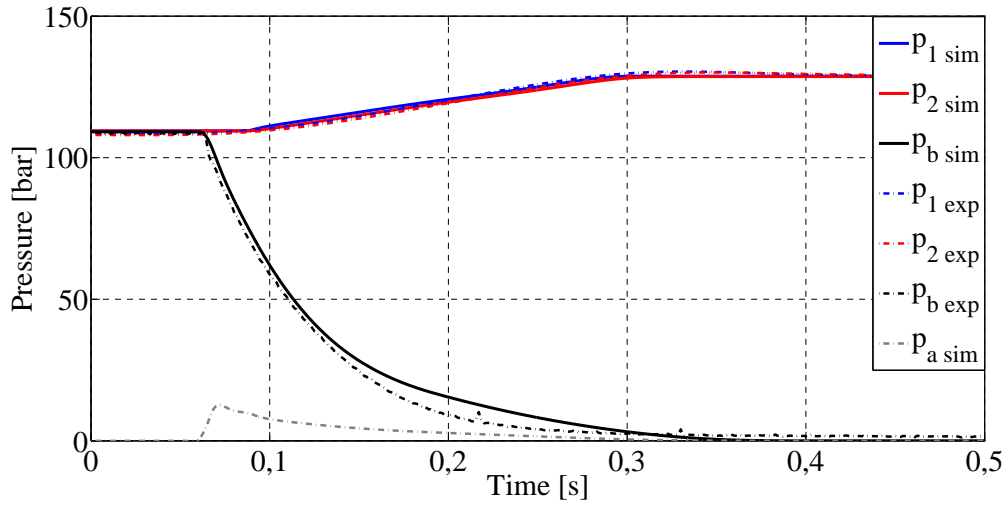


Fig. 6. 'Falling phase': 1= 1st TMC chamber, 2= 2nd TMC chamber, b= Rear Right caliper, a= accumulator, exp=experimental, sim= simulation

electro-mechanical system is characterized by saturation in both directions: for a DC lower than 30% the valve behaves as a fully open one and for DC greater than 55% the valve works as a fully closed one. Based on this consideration, inlet and outlet valves can be modeled with second-order transfer functions with a non constant static gain as indicated in Eq. 14. The dynamic parameters σ_n and ζ are roughly derived through a curve-fitting procedure between the simulated pressure trend and the experimental results for a specific DC, as indicated in Fig. 8. The figure also makes clear the effect of the PWM frequency on the pressure ripple: while the outlet valve PWM frequency of 50 Hz is close to its natural frequency amplifying pressure oscillations, the high value of inlet valve modulation frequency of 900 Hz is very well attenuated due to the mechanical low pass filtering effect involved by the valve dynamics.

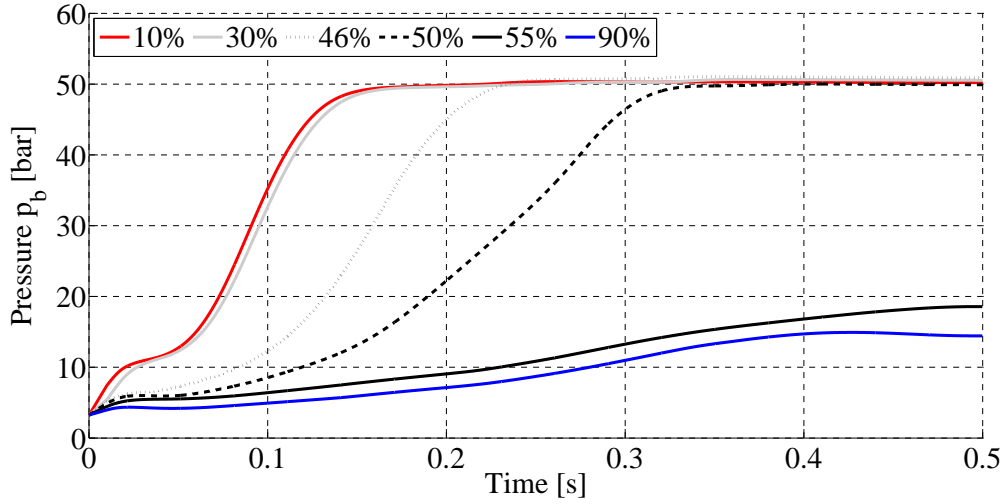


Fig. 7. Effect of PWM Duty Cycle on pressure trend in the brake caliper: the inlet valve is controlled via a constant frequency and variable Duty Cycle

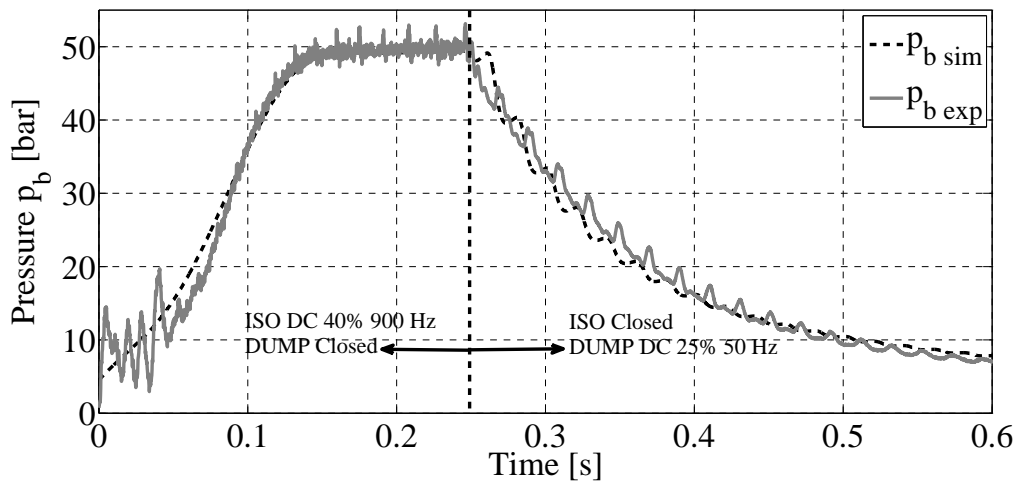


Fig. 8. Raising and falling phases by applying a PWM signal of 40% DC and modulation frequency of 900 Hz to the inlet valve and a PWM signal of 25% DC on 50 Hz to the outlet valve

The variable static gain G_s , which takes into account all the unmodeled non-linearities, e.g. introduced by the relay box and electro-mechanics behavior of valves, is identified from experimental curve-fitting all over the effective DC range (e.g. from 30% to 55% for the inlet valve) finally getting the non-linear static behavior between DC and effective flow area A_i shown in Fig. 9. The inlet valve gain shows a monotonically decreasing trend which has a clear physical meaning since it states that when Duty Cycle increases the inlet valve behaves as a closed valve. On the other hand, the outlet valve gain is characterized by an increasing trend followed, after the maximum, by a decreasing trend and thus showing a different behavior from the inlet valve, also because of the motor-pump presence.

V. MODEL VALIDATION

This last section presents the experimental validation of the non-linear model by applying the same time-histories used during specific experimental tests in order to compare simulated brake pressure behavior with the pressure measured by sensors. Two different time-histories are chosen to be as close as possible to real operating conditions of vehicle braking system:

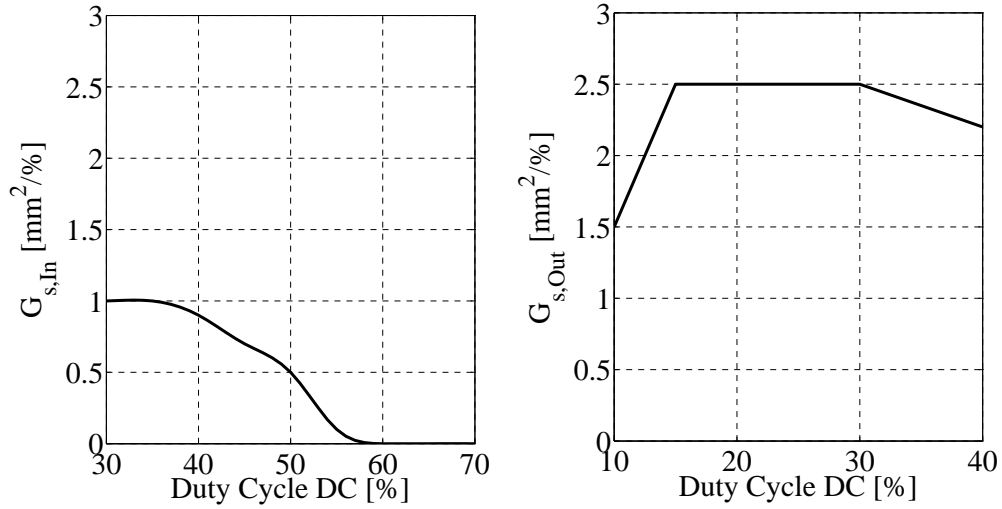


Fig. 9. Static Gain G_s for both inlet (left) and outlet (right) valve

- Normal production ABS emergency wheel anti-lock control strategy
- PWM signal with variable Duty Cycle for both inlet and outlet valves

In the first case, both test rig and non-linear model receive the same input coming from a real emergency braking maneuver where the system is activated in order to avoid wheel locking. An example of valves activation is reported in Fig. 10 (activation of outlet valve always comes together with motor-pump to empty brake calipers) together with the comparison of brake caliper pressures obtained during simulation and from test rig sensors. A proper tuning of the inlet valve static gain, focused on low pressures, has led to a good estimation in that range: the RMS value of the error between simulation and experimental data in the time range shown in Fig. 10 is 1.5 bar.

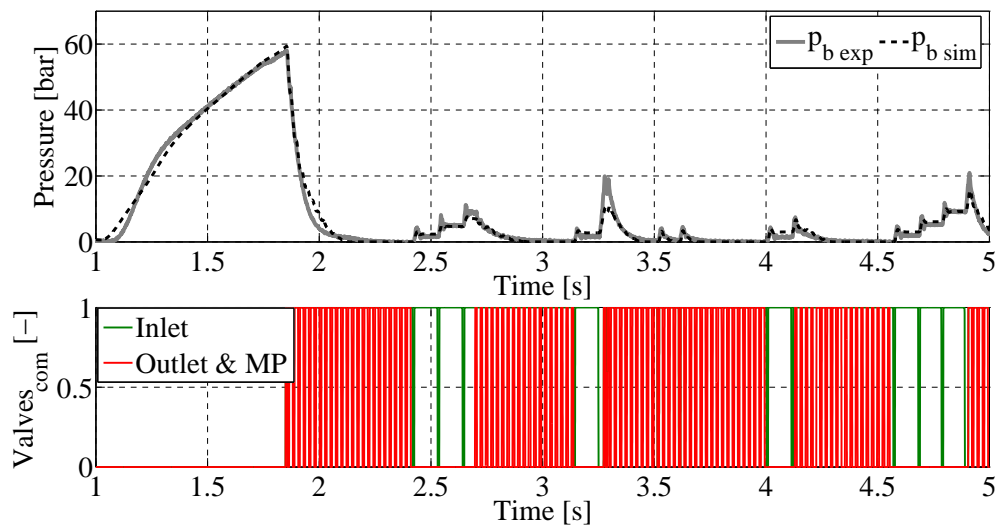


Fig. 10. Experimental validation of non-linear model during ABS emergency braking under extremely low road friction conditions: b= Rear Right caliper, exp=experimental, sim= simulation

Finally, a more specific test is elaborated for evaluating valves dynamic response to a PWM signal with a constant frequency and variable Duty Cycle. The time history is chosen in order to cover the whole range where Duty Cycle is effective on the

pressure gradient as described in the previous section. The simulation has been carried out by adding to both valves input commands a time delay equal to the sampling period (0.02 s) used during experimental test. Contrary to the other tests, where the sampling frequency is 10 kHz, in this case (frequency of 50 Hz) the time delay due to the sampling period cannot be neglected. Fig. 11 reports the experimental validation showing a good match between experimental and simulated brake pressure (RMS error is 3.5 bar), especially during the activation of inlet valve.

The RMS value of the error between experimental and simulation data is lower in the case of ABS emergency test than the PWM signal test due to a lower mean value (10 bar and 35 bar respectively).

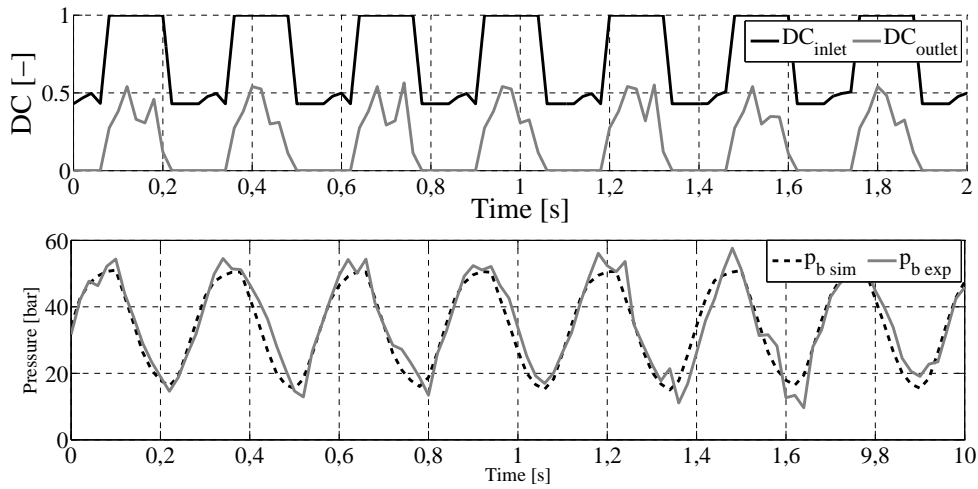


Fig. 11. Experimental Validation of Non-Linear Model under a PWM signal excitation: b= Rear Right caliper, exp=experimental, sim= simulation

VI. CONCLUSIONS

Conclusion of the first part of this activity can be summarized as follow:

- a normal production hydraulic circuit mounted on passenger cars has been modeled by a non-linear model which takes into account TMC longitudinal dynamics, pressure dynamics inside brake caliper/TMC chambers, oil compressibility as a function of its pressure and its relative gas content, non-linear behavior of valve electro-mechanical command and the presence of a motor-pump with a spring accumulator.
- all parameters of the model have been identified from experimental data acquired from a HIL test bench characterized by a real passenger car hydraulic system with a ABS/ESC customized unit and a real-time data acquisition system.
- for a better analysis of valves dynamic behavior, a PWM signal with a fixed frequency and variable DC is applied to inlet and outlet valves.
- the mathematical model here presented and experimentally validated represents a valid tool for the analysis of specific control strategies as will be addressed in the second part of this activity.

VII. LIST OF SYMBOLS

- 1 : subscript relative to first TMC chamber
 2 : subscript relative to second TMC chamber
 a : subscript relative to spring accumulator
 A_i : flow area of i^{th} hydraulic resistance
 b : subscript relative to Rear-Right brake caliper
 b_i : damping coefficient of the i^{th} hydraulic chamber
 $c_{q,i}$: flow Coefficient relative to i^{th} flow rate
 $c_{q,max}$: max flow Coefficient
 DC : Duty Cycle of a PWM signal
 eq : subscript relative to the equivalent hydraulics circuit composed by Front Right and Rear Left calipers
 F_{fi} : Friction force actiong on the i^{th} element
 FL : subscript relative to Front Left brake caliper
 G_s : static gain of second-order valves dynamics
 h_d : hydraulic diameter
 In : subscript relative to inlet valve
 k_i : stiffness of i^{th} spring
 m_i : mass of i^{th} element
 n : gas-specific heat ratio
 Out : subscript relative to outlet valve
 p : subscript relative to pump
 p_i : pressure of i^{th} hydraulic branch
 Q_i : flow rate across the i^{th} hydraulic resistance
 s : Laplace variable
 S : TMC hydraulic cylinder surface
 S_a : spring accumulator hydraulic surface
 TMC : Tandem Master Cylinder
 U : Valves input voltage
 V_i : volume of i^{th} hydraulic capacity
 x_i : position of i^{th} element
 α : oil relative gas content at atmospheric pressure
 β : oil + pipe equivalent bulk modulus
 β_n : oil pure liquid bulk modulus
 Δp_i : pressure drop across the i^{th} valve
 ζ : damping factor of second-order valves dynamics

λ_{cr} : critical flow number

ρ : oil density

σ_n : natural frequency of second-order valves dynamics

ν : oil kinematic viscosity

APPENDIX

TABLE I
MODEL PARAMETERS

Symbol	Description	Value
A_{In}	Inlet valve flow Area	$0.29mm^2$
A_{Out}	Outlet valve flow Area	$0.59mm^2$
b_1, b_2	TMC viscous damping coefficient	$100Nms/rad$
b_a	Accumulator damping coefficient	$85Nms/rad$
$c_{q,max}$	Max Flow Coefficient	0.7
F_{f2}	TMC Friction Force	$14N$
F_{fa}	Accumulator Friction Force	$0N$
k_1	First Spring Stiffness	$2222.2N/m$
k_2	Second Spring Stiffness	$4000N/m$
k_a	Accumulator Spring Stiffness	$35N/m$
m_2	Second TMC Mass	$40g$
m_a	Accumulator Mass	$10g$
n	Gas specific heat ratio	1.4
p_{th}	Pressure threshold for Pump Flow Rate	$0.6bar$
Q_{ss}	Pump Flow Rate	$0.26l/min$
S	TMC Thrust Surface	$5.07cm^2$
S_a	Accumulator Thrust Surface	$2.54cm^2$
V_{10}	First TMC Volume Chamber	$18.8cm^3$
V_{20}	Second TMC Volume Chamber	$12.5cm^3$
V_b	Brake Volume	$338.9cm^3$
α	Relative gas content at atmospheric pressure	0.02
β_n	Pure Liquid Bulk Modulus	$27000bar$
ζ	Damping ratio of electro-mechanics valve	35%
λ_{cr}	critical flow number	100
ρ	Oil Density	$1070kg/m^3$
σ_n	Natural frequency of electro-mechanics valve	$251rad/s$
ν	Kinematic viscosity	$100e^{-6}kg/(ms)$

REFERENCES

- [1] R. Bosch. GmbH, *Bosch Automotive Handbook*, 7th ed. Plochingen, Germany, 2007.
- [2] R. Bosch. GmbH, *Anti-lock brakes system specification*, Plochingen, Germany, 2005.
- [3] J. Zhang, C. Lv, X. Yue, Y. Li, Y. Yuan, *Study on a linear relationship between limited pressure difference and coil current of on/off valve and its influential factors*, ISA Transactions, Volume 53, Issue 1, January 2014, Pages 150-161.
- [4] F. Cheli, A. Concas, E. Giangiulio, E. Sabbioni, *A simplified ABS numerical model: Comparison with HIL and full scale experimental tests*, Computers & Structures, Volume 86, Issues 1314, July 2008, Pages 1494-1502.
- [5] D. Capra, E. Galvagno, V. Ondrak, B. van Leeuwen, A. Vigliani, *An ABS control logic based on wheel force measurement*, Vehicle System Dynamics, Volume 50(12), 2012, Pages 1779-1796.
- [6] A. Morgando, M. Velardocchia, A. Vigliani, V. Ondrak, B. van Leeuwen, *An alternative approach to automotive ESC based on measured wheel forces*, Vehicle System Dynamics, Volume 49(12), 2011, Pages 1855-1871.
- [7] M. Wu, M. Shih, *Simulated and experimental study of hydraulic anti-lock braking system using sliding-mode PWM control*, Mechatronics, Volume 13, Issue 4, May 2003, Pages 331-351.
- [8] Y. Khan, P. Kulkarni, K. Youcef-Toumi, *Modelling Experimentation and Simulation of a Brake Apply System*, American Control Conference, 24-26 June 1992, Pages 226-230.
- [9] B. Ozdalyan, M.V. Blundell, *Anti-lock braking system simulation and modelling in ADAMS*, International Conference on Simulation '98 (Conf. Publ. No. 457) , 30 Sep-2 Oct 1998, Pages 140-144.
- [10] D. V. Tretyak, S. V. Kliuzovich, K. Augsborg, J. Sandler, and V. G. Ivanov *Research in hydraulic brake components and operational factors influencing the hysteresis losses* Proceedings of the Institution of Mechanical Engineers, Part D: Journal of Automobile Engineering, 1 September 2008, Pages 1633-1645.
- [11] J. R. Valds, J. M. Rodriguez, J. Saumell, T. Ptz, *A methodology for the parametric modelling of the flow coefficients and flow rate in hydraulic valves*, Energy Conversion and Management, Volume 88, December 2014, Pages 598-611.
- [12] S. Baek, J. Song, D. Yun, H. Kim, K. Boo, *Application of a sliding mode control to anti-lock brake system*, International Conference on Control, Automation and Systems, 14-17 Oct. 2008, Pages 307-311.
- [13] B. Moaveni, P. Barkhordari, *Identification and characterization of the hydraulic unit in an anti-lock brake system*, Proceedings of the Institution of Mechanical Engineers, Part D: Journal of Automobile Engineering, 4 November 2015, Pages 1-11.
- [14] H. Raza, Z. Xu, B. Yang, P.A. Ioannou, *Modeling and control design for a computer-controlled brake system*, IEEE Transactions on Control Systems Technology, Volume 5, no.3, May 1997, Pages 279-296.
- [15] M. Taghizadeh, A. Ghaffari, F. Najafi, *Modeling and identification of a solenoid valve for PWM control applications*, Comptes Rendus Mecanique, Volume 337, Issue 3, March 2009, Pages 131-140.
- [16] M. Velardocchia, A. Sornioti, *Hardware-In-the-Loop to Evaluate Active Braking System Performance*, SAE Technical Paper, 2005-01-1580, 2005.
- [17] D. McCLOY, H. MARTIN, *Control of Fluid Power : Analysis and design*, 2nd edition, Ellis Horwood Limited, 1980.
- [18] R. Petrovi, R. ivkovi, M. Rong, W. Z. Raki, R. Slavkovi, *Influence of Air Content Entrained in Fluid of a Vane Pump with Double Effect Operating Parameters*, Tehniki vjesnik - Technical Gazette, vol. 21, no. 2, p. 401-407, 2014.